

# Mamba as Decision Maker: Exploring Multi-scale Sequence Modeling in Offline Reinforcement Learning

Jiahang Cao<sup>1\*</sup> Qiang Zhang<sup>1\*</sup> Ziqing Wang<sup>2</sup> Jingkai Sun<sup>1</sup> Jiaxu Wang<sup>1</sup> Hao Cheng<sup>1</sup>  
Yecheng Shao<sup>4</sup> Wen Zhao<sup>3</sup> Gang Han<sup>3</sup> Yijie Guo<sup>3</sup> Renjing Xu<sup>1†</sup>

<sup>1</sup>The Hong Kong University of Science and Technology (Guangzhou)

<sup>2</sup>Northwestern University

<sup>3</sup>Beijing Innovation Center of Humanoid Robotics

<sup>4</sup>Center for X-Mechanics, Zhejiang University

**Abstract:** Sequential modeling has demonstrated remarkable capabilities in offline reinforcement learning (RL), with Decision Transformer (DT) being one of the most notable representatives, achieving significant success. However, RL trajectories possess unique properties to be distinguished from the conventional sequence (*e.g.*, text or audio): (1) local correlation, where the next states in RL are theoretically determined solely by current states and actions based on the Markov Decision Process (MDP), and (2) global correlation, where each step’s features are related to long-term historical information due to the time-continuous nature of trajectories. In this paper, we propose a novel action sequence predictor, named Mamba Decision Maker (MambaDM), where Mamba is expected to be a promising alternative for sequence modeling paradigms, owing to its efficient modeling of multi-scale dependencies. In particular, we introduce a novel mixer module that proficiently extracts and integrates both global and local features of the input sequence, effectively capturing interrelationships in RL datasets. Extensive experiments demonstrate that MambaDM achieves state-of-the-art performance in Atari and OpenAI Gym datasets. Furthermore, we empirically investigate the scaling laws of MambaDM, finding that increasing model size does not bring performance improvement, but scaling the dataset amount by  $2\times$  for MambaDM can obtain up to 33.7% score improvement on Atari dataset. This paper delves into the sequence modeling capabilities of MambaDM in the RL domain, paving the way for future advancements in robust and efficient decision-making systems. Our code will be available at <https://github.com/AndyCao1125/MambaDM>.

**Keywords:** Offline Reinforcement Learning, Mamba

## 1 Introduction

Decision-making in Reinforcement Learning (RL) typically involves learning a mapping from state observations to actions that maximize cumulative discounted rewards. Recently, Chen et al. [1] introduced the Decision Transformer (DT), which leverages the simplicity and scalability of transformer architectures to establish a new paradigm for learning in offline RL. DT reinterprets the decision-making process as a sequence modeling problem, learning a return-conditioned state-action mapping. This approach predicts the necessary action to achieve a desired return based on a sequence of past returns, states, and actions. Due to its promising performance, this sequence modeling paradigm has been widely applied to various robotics tasks, including manipulation [2, 3], navigation [4], and behavior generation [5].

---

\*Equal contribution.

†Corresponding author.

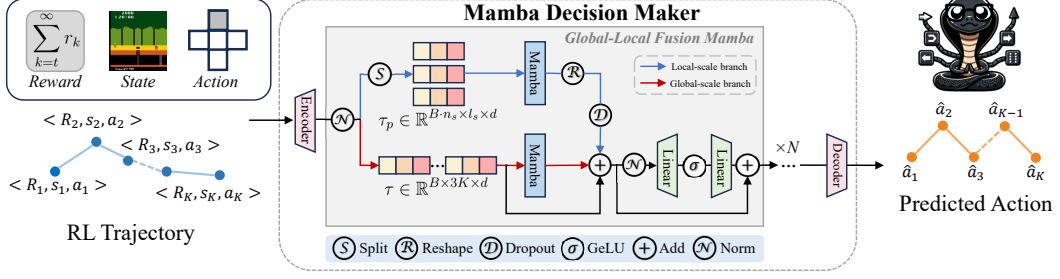


Figure 1: Overview of our method. The input RL trajectory is first processed by the embedding layers, and these embeddings are then passed through both local and global branches to extract multi-scale features. Subsequently, the combined information from these branches is fed into a feed-forward network (FFN). After passing through  $N$  layers, the final action sequence is obtained by the action predictor.

However, RL trajectories differ from conventional sequences like text or audio, and thus modeling them cannot be treated as a simple sequence modeling task. RL problems are typically defined by a Markov Decision Process (MDP), where state transition probabilities adhere to the Markov property—meaning the probability of transitioning to the next state depends solely on the current state and action, not on past states. Consequently, local correlations between steps in the trajectory sequence are significant and cannot be ignored. Additionally, since time steps are sequential, each step’s features are related to long-term history information, indicating that RL trajectories also exhibit inner global correlations. Therefore, designing a multi-scale model to capture both global and local features of RL trajectories deserves further exploration.

In this paper, we introduce the Mamba Decision Maker (MambaDM), which provides an in-depth study of the effectiveness of the Mamba module within the framework of reward conditional sequence modeling. We innovatively design the Global-local fusion Mamba (GLoMa) module to capture both local and global features to better understand the inner correlations within RL trajectories, aiming to enhance model performance. Furthermore, we explore the scaling laws of MambaDM in RL tasks. Unlike in NLP, where larger models typically yield better performance, our findings indicate that, in Atari and OpenAI Gym environments, increasing model size does not necessarily enhance results. But providing a larger datasize for MambaDM can bring performance improvement. We also analyze the Mamba module’s ability to capture dependency information by visualizing changes in the eigenvalues of Mamba’s core transition matrix. Extensive experiments demonstrate that MambaDM achieves state-of-the-art performance across multiple tasks, significantly outperforming the Decision Transformer (DT [1]) in Atari and OpenAI Gym task, and exceeding the performance of state space model-based [6, 7] DMamba [8] by up to 75.3%.

Our contributions can be summarized as follows:

- We propose the Mamba Decision Maker (MambaDM), an effective decision-making method that incorporates a novel global-local fusion mamba (GLoMa) module to model RL trajectories from both global and local perspectives.
- We investigate the scaling laws of MambaDM in RL tasks. Our experimental results indicate that the scaling laws of MambaDM do not completely align with those observed in NLP, suggesting that gathering larger and more diverse RL datasets could be a more effective strategy for enhancing performance compared to merely increasing the model size.
- Extensive experiments validate that MambaDM achieves state-of-the-art results in Atari and OpenAI Gym, significantly outperforming state space model-based DS4 and DMamba. Additionally, our visualization analysis demonstrates MambaDM’s ability to capture both short-term and long-term dependencies, supporting the reliability of the proposed module.

## 2 Related Work

### 2.1 Offline Reinforcement Learning

Reinforcement Learning (RL) is a framework of algorithms that learn through interactions with an environment. The problem is formulated as a Markov Decision Process [9, 10]. Reinforcement Learning aims to maximize rewards through interactions with an environment, which is often a time-consuming and expensive process. Drawing inspiration from supervised learning, researchers have explored offline reinforcement learning as a means to circumvent the traditional paradigm of online interactions [11, 12]. Compared to online reinforcement learning, which involves interacting with the environment, offline reinforcement learning more closely resembles a data-driven paradigm as it relies on the offline dataset. Researchers have developed various approaches to offline reinforcement learning. Including methods based on value functions [12, 13], uncertainty quantification [14, 15, 16], dynamics estimation [17, 17, 18, 19, 20] and conditional behavior cloning that avoid value functions [21, 22, 23, 24, 25, 26, 27]. These investigations into offline reinforcement learning have extensively explored the utilization of offline data, thereby stimulating further scholarly contemplation on leveraging such data for reinforcement learning applications.

### 2.2 Sequence Modeling for Offline Reinforcement Learning

As supervised learning continues to evolve, sequence models have achieved significant success in many research areas. Given the structural similarities between RL’s Markov processes and sequence modeling, many researchers have begun to consider integrating sequence models with RL. The Decision Transformer (DT) [1] employs a Transformer to convert an RL problem into a sequence modeling task and treats a trajectory as a sequence of rewards, states, and actions. Max et al. [28] discuss the role of the attention mechanisms in DT, offering various opinions and motivating us to employ advanced sequence modeling techniques. Decision Convformer [29] incorporates discussions from the computer vision field about the MetaFormer [30] structure for transformers and proposes considerations for the use of local features. However, the structure in DC focuses too much on local information and structures, which can impact the utilization of global information. Decision S4 [31] uses S4 layers for sequence modeling in offline RL. Decision Mamba [8] integrates the latest Mamba sequence model. However, both methods merely apply these new sequence models directly without further exploring and utilizing the potential of these sequence models. In this paper, we introduce MambaDM, an innovative sequence modeling framework designed for offline RL. MambaDM integrates the unique features of state space models to effectively combine local and global features, enhancing learning capabilities and efficiently handling larger-scale training.

## 3 Preliminaries

### 3.1 RL Problem Setup

An RL problem can be modeled as a Markov decision process (MDP)  $\mathcal{M} = \langle \rho_0, \mathcal{S}, \mathcal{A}, P, \mathcal{R}, \gamma \rangle$ , where  $\rho_0$  represents the initial state distribution,  $\mathcal{S}$  is the state space, and  $\mathcal{A}$  is the action space. At timestep  $t$ , a specific state and action are denoted by  $s_t$  and  $a_t$ , respectively. The transition probability  $P(s_{t+1}|s_t, a_t)$  adheres to the Markov property. The reward function  $\mathcal{R}$  provides the reward  $r_t = \mathcal{R}(s_t, a_t)$ , and  $\gamma \in (0, 1)$  is the discount factor. We utilize the return-to-go (RTG, *i.e.*,  $\hat{R}_t = \sum_{k=t}^{\infty} \gamma^k r_k$ ) as the reward input, following the approach of the Decision Transformer. Given an offline RL trajectory dataset, our objective is to determine an optimal policy  $\pi^*$  that predicts the best actions to maximize the expected return by interacting with the environment.

### 3.2 State Space Model

The state space models (SSMs) are a recent class of sequence models inspired by a particular dynamic system. SSMs map a 1-dimensional (1D) input  $x(t) \in \mathbb{R}$  to the output signal  $y(t) \in \mathbb{R}$  through an implicit latent  $h(t) \in \mathbb{R}^N$ . Concretely, we provide a detailed definition of structure state space models (S4) to illustrate the modeling process:

$$h'(t) = Ah(t) + Bx(t), \quad (1)$$

$$y(t) = Ch(t) + Dx(t), \quad (2)$$

where  $(A, B, C, D)$  controls the whole continuous system, and  $A$  acts as an important state matrix which strongly decides the ability to capture long-range dependencies by different HIPPO initialization [32]. To operate discrete sequences, S4 needs to be transformed into a discretized form:

$$h'(t) = \overline{A}h(t) + \overline{B}x(t), \quad (3)$$

$$y(t) = Ch(t), \quad (4)$$

where S4 uses the zero-order hold (ZOH) discretization rule:  $\overline{A} = \exp(\Delta A)$  and  $\overline{B} = (\Delta A)^{-1}(\exp(\Delta A) - I)(\Delta B)$ .  $D$  can be considered as parameter-based skip connections, thus we simplify  $D$  as 0. After transforming from  $(\Delta, A, B, C, D) \mapsto (\overline{A}, \overline{B}, C)$ , the model can be computed in two ways: (a) linear recurrence view which only needs  $O(1)$  complexity during inference, and (b) global convolution view that achieves fast parallelizable speed during training. This deformable nature gives SSM a remarkable lightweight advantage over classical sequence models such as transformer [33] and RWKV [34] in NLP tasks.

### 3.3 Mamba

To further enhance selectivity and context-aware capabilities, Mamba [7] is proposed to handle complex sequence tasks by expanding the embedding space while maintaining efficient implementation. Building on the S4 structure, Mamba transitions the main parameters from time-invariant to time-varying. Additionally, the architecture of the Mamba block integrates elements from both H3 [35] and gated MLP [36, 37], making it versatile for incorporation into neural networks. Recent extensive research demonstrates that Mamba significantly contributes to various tasks, including but not limited to, vision [38, 39, 40], language [41, 42], and medical [43, 44] domains.

## 4 Methodology

### 4.1 Overview

The overview of our method is presented in Figure 1. We propose a global-local fusion mamba (GLoMa) framework where the input trajectory is processed jointly by multi-scale branches. This design ensures that both global and local features are effectively leveraged for optimal performance.

### 4.2 Motivation and Insights

As mentioned before, RL trajectories differ from conventional sequences with two unique properties: (1) local correlations and (2) global correlations. In this paper, we adopt the Mamba model [7], known for its efficient sequence modeling and strong ability to capture multi-scale dependencies [6], to explore its capability to model the inner relationship of RL trajectories. We develop the global-local fusion mamba (GLoMa) module to effectively integrate local features and global features. Inspired by transformer-in-transformer (TNT [45]), which aims to extract finer-grained features, S-MNM focuses on fusing global and local features within trajectories, differing from TNT’s focus on combining with more granular image texture features.

### 4.3 Mamba Decision Maker

**Global-local fusion Mamba (GLoMa).** Given a sequence of trajectories  $\tau_{\text{raw}}$  sampled from dataset  $D$  with raw RTG, state, and action, we first obtain the trajectory representation  $\tau$  through the token embedding layer:

$$\tau = \text{Emb}(\tau_{\text{raw}}) = (\langle \hat{R}_1, s_1, a_1 \rangle, \langle \hat{R}_2, s_2, a_2 \rangle, \dots, \langle \hat{R}_K, s_K, a_K \rangle) \in \mathbb{R}^{3K \times d} \quad (5)$$

where  $K$  is the context length,  $d$  is the embedding dimension. Then, the trajectory sequence  $\tau$  is processed by both the global and local branches. For the local branch, the input sequence is evenly divided into sub-sequences, each of length  $l_s$ . Since the total sequence length is fixed with  $3K$ , it might lead to uneven sub-sequence lengths. To address this, we pad zeros at the end of the sequence to ensure uniform length and generate the sub-sequences through:

$$l_p = (l_s - (3K \bmod l_s)) \bmod l_s, \quad (6)$$

$$\tau_p = g_s(\text{Pad}(\tau, l_p), l_s) \in \mathbb{R}^{n_s \times l_s \times d} \quad (7)$$

Scaling Factor	Context Length	Layer Number	Embedding Dimension	Dataset Size
Range	(10, 30, 50, 80, 100)	(3, 6, 8, 12)	(128, 256, 512)	(250K, 500K, 1M)

Table 1: Experimental settings for scaling factors in MambaDM.

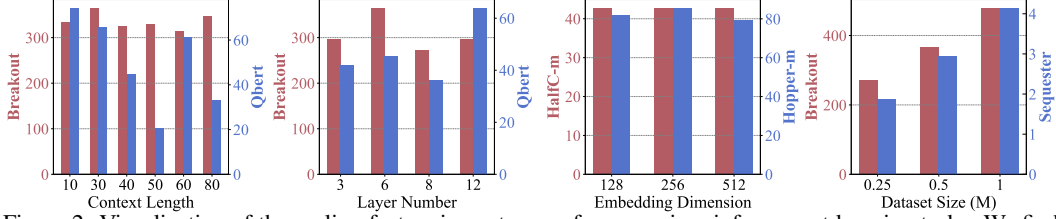


Figure 2: Visualization of the scaling factors impact on performance in reinforcement learning tasks. We find that increasing the dataset size can significantly improve the model’s performance.

where  $l_p$  denotes the padding length,  $n_s = \frac{3K+l_p}{l_s}$  denotes the number of sub-sequences.  $\text{mod}$  and  $\text{Pad}$  means the modulo and padding operator, respectively.  $g_s(\cdot)$  denotes the split function, which splits the input into  $l_s$ -length sequences. The  $n_s$  dimension will be merged with the batch dimension during training. We can then obtain the local-scale feature of sub-sequences through the Mamba module by Equation 8. For the global branch, we model the entire sequence directly using the Mamba block with Equation 9. Overall, this multi-scale process can be formulated by:

$$f_{\text{local}} = \text{Mamba}(\text{LN}(\tau_p)), \quad (8)$$

$$f_{\text{global}} = \text{Mamba}(\text{LN}(\tau)), \quad (9)$$

where  $\text{LN}$  denotes the layer normalization. The multi-scale feature  $f_c$  is combined with a Dropout layer [46] and then fed into an FFN layer to obtain the output features:

$$f_c = f_{\text{global}} + \text{Dropout}(f_{\text{local}}) \quad (10)$$

$$f = \text{FFN}(\text{LN}(f_c)) + f_c \quad (11)$$

After passing through  $L$  layers of the network, the final features  $f_L$  are input into the prediction head to predict the action sequence:  $\hat{a}_t = \text{Head}(f_L)$  with  $t = 1, 2, \dots, K$ .

By implementing these techniques, our Global-local fusion mamba (GLoMa) framework aims to effectively capture and integrate both local and global features to better understand the inner correlations within RL trajectories, enhancing the model’s ability to predict action sequences accurately.

**Training and Inference.** In the training stage, considering the true-optimal action as  $a_t^*$ , the training object is to minimize the loss between the predicted action  $\hat{a}_t$  and true action  $a_t^*$ :

$$\mathcal{L} = \begin{cases} \mathbb{E}_{\tau_{\text{raw}} \sim D} [\|a_t^* - \hat{a}_t\|^2], & \text{if action is continuous;} \\ \mathbb{E}_{\tau_{\text{raw}} \sim D} [-a_t^* \log(\hat{a}_t)], & \text{if action is discrete.} \end{cases} \quad (12)$$

In this paper, the actions in the Atari benchmark [47] are discrete, whereas those in D4RL [48] are continuous. During inference, the final action  $a_K$  is unknown. To handle the variable length of the input sequence, we set  $l_s$  to match its length. Additionally, the true RTG is unavailable. Therefore, following Chen et al. [1], we set the target RTG to be the initial RTG. We find that the initial RTG significantly affects the final results, and we discuss this phenomenon in Section 5.5.

## 5 Experiments

### 5.1 Exploring the Scaling Laws of MambaDM

In this section, we investigate the scaling laws of MambaDM within the context of reinforcement learning (RL) tasks. Scaling laws [49], as observed in the natural language processing (NLP) domain, suggest that increasing computational resources generally leads to improved performance. Our objective is to explore if similar scaling laws apply to MambaDM when used for RL tasks.

**Experiment Setting.** To systematically study this, we conduct a series of experiments varying key parameters of MambaDM. Specifically, we manipulate the context length, layer number, embedding

Game	CQL	BC	DT	DC	DC <sup>hybrid</sup>	DMamba <sup>†</sup>	MambaDM
Breakout	211.1	142.7	242.4 ± 31.8	352.7 ± 44.7	<b>416.0 ± 105.4</b>	239.2 ± 26.4	<b>365.4 ± 20.0</b>
Qbert	104.2	20.3	28.8 ± 10.3	<b>67.0 ± 14.7</b>	62.6 ± 9.4	42.3 ± 8.5	<b>74.4 ± 8.4</b>
Pong	111.9	76.9	105.6 ± 2.9	106.5 ± 2.0	<b>111.1 ± 1.7</b>	63.2 ± 102.1	<b>110.8 ± 2.3</b>
Seaquest	1.7	2.2	<b>2.7 ± 0.7</b>	2.6 ± 0.3	<b>2.7 ± 0.04</b>	2.2 ± 0.03	<b>2.9 ± 0.1</b>
Asterix	4.6	4.7	5.2 ± 1.2	<b>6.5 ± 1.0</b>	6.3 ± 1.8	5.5 ± 0.3	<b>7.5 ± 1.4</b>
Frostbite	9.4	16.1	25.6 ± 2.1	27.8 ± 3.7	<b>28.0 ± 1.8</b>	25.3 ± 1.5	<b>33.7 ± 4.4</b>
Assault	73.2	62.1	52.1 ± 36.2	73.8 ± 20.3	<b>79.0 ± 13.1</b>	67.2 ± 6.9	<b>81.4 ± 3.1</b>
Gopher	2.8	33.8	34.8 ± 10.0	<b>52.5 ± 9.3</b>	51.6 ± 10.7	27.0 ± 3.9	<b>54.4 ± 11.1</b>

Table 2: Comparisons results of MambaDM and baselines in the Atari datasets. The gamer-normalized returns are reported, following Ye et al. [50], and averaged across three random seeds. The top-1 and top-2 results among the DT variants are highlighted in **deep pink** and **light pink**, respectively. <sup>†</sup> denotes that we reproduce the DMamba’s results of the last four games (in gray) which are not provided in the origin paper.

Dataset	Env.	TD3+BC	IQL	CQL	RvS	DT	DS4	DMamba	MambaDM
<i>M</i>	halfcheetah	48.3	47.4	44.0	41.6	<b>42.6</b>	42.5	<b>42.8</b>	<b>42.8 ± 0.1</b>
	hopper	59.3	63.8	58.5	60.2	68.4	54.2	<b>83.5</b>	<b>85.7 ± 7.8</b>
	walker2d	83.7	79.9	72.5	71.7	75.5	<b>78.0</b>	<b>78.2</b>	<b>78.2 ± 0.6</b>
<i>M-R</i>	halfcheetah	44.6	44.1	45.5	38.0	37.0	15.2	<b>39.6</b>	<b>39.1 ± 0.1</b>
	hopper	60.9	92.1	95.0	73.5	<b>85.6</b>	49.6	82.6	<b>86.1 ± 2.5</b>
	walker2d	81.8	73.7	77.2	60.6	<b>71.2</b>	69.0	70.9	<b>73.4 ± 2.6</b>
<i>M-E</i>	halfcheetah	90.7	86.7	91.6	92.2	88.8	<b>92.7</b>	<b>91.9</b>	86.5 ± 1.2
	hopper	98.0	91.5	105.4	101.7	109.6	<b>110.8</b>	<b>111.1</b>	110.5 ± 0.3
	walker2d	110.1	109.6	108.8	106.0	<b>109.3</b>	105.7	108.3	<b>108.8 ± 0.1</b>

Table 3: Comparisons results of MambaDM and baselines in D4RL benchmark with Medium (M), Medium-Reply (MR) and Medium-Expert (ME) datasets. We report the expert-normalized returns, following Fu et al. [48], averaged across three random seeds. The top-1 and top-2 results among the DT variants are colored in **deep pink** and **light pink**, respectively.

dimension, and dataset size. The settings for these parameters are chosen to cover a broad range of values and to provide a comprehensive understanding of their impact on performance. The details of these settings are illustrated in Table 1.

**Discussion.** In our investigation of the scaling law in MambaDM for RL tasks, we explore how variations in scaling factors affect performance, as depicted in Figure 2. Our findings indicate that MambaDM does not exhibit NLP-like scaling behaviors in Atari and OpenAI Gym. As we increase the model size, performance fluctuations are observed instead of a clear upward trend. Consequently, **MambaDM does not demonstrate a definitive scaling law when scaling the model size.** However, our experiments show that **increasing the dataset size can significantly improve the model’s performance.** This suggests that focusing on gathering larger and more diverse RL datasets could be a more effective strategy for enhancing performance compared to merely increasing the model size in Atari and OpenAI Gym. We delve into the reasons why MambaDM does not exhibit an NLP-like scaling law in Appendix A.2.

## 5.2 Evaluations on Atari Games

**Baselines.** We choose six models as our baselines, including temporal difference learning methods: Conservative Q-Learning (CQL [13]), imitation learning methods: Behavior Cloning (BC [51]), Decision Transformer (DT [1]), Decision ConvFormer (DC [29]) and Decision Mamba (DMamba [8]).

**Experiment Setting.** To ensure a fair comparison, we adopt the same model hyperparameter settings as those used in DT and DC. All experimental settings are detailed in the Appendix to ensure reproducibility. The experimental results for the baselines are from DC and DMamba. Each experimental result is the average of three runs with different random seeds. We conduct eight discrete control tasks from the Atari domain. Each experiment is conducted on a single NVIDIA 4090 GPU.

**Comparisons with the State-of-the-art.** As illustrated in Table 2, our proposed MambaDM has a significant improvement across different Atari games. For instance, MambaDM’s performance



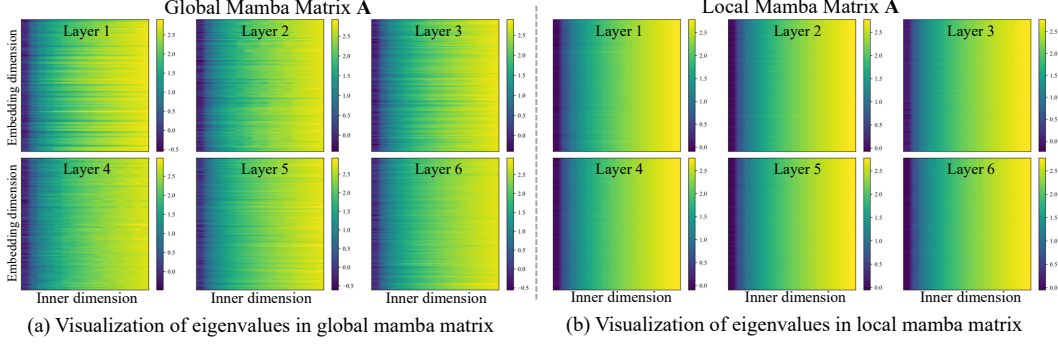


Figure 3: Visualization of the eigenvalues in our proposed S-MNM module, including (a) global mamba and (b) local mamba block.

on Qbert significantly improved by 45.6% and 32.1% compared with DT and DMamba. When compared with the latest state-of-the-art method DC, MambaDM achieves favorable gains across all games. These results demonstrate the effectiveness of our method in the discrete Atari domain.

### 5.3 Evaluations on OpenAI Gym

**Baselines.** Seven models are chosen as our baselines, including TD3+BC [52], IQL [53], RvS [27], DT [1] and two state space model-based [6] approaches: DS4 [31] and DMamba [8].

**Experiment Setting.** We adopt the same model hyperparameter settings as those used in DT and DC for fair comparisons. We conduct experiments in three different MuJoCo domains [48]: halfcheetah, hopper, and walker, where each environment has three quality levels, including medium (M), medium-replay (M-R) and medium-expert (M-E).

**Comparisons with the State-of-the-art.** Table 3 presents a performance comparison of MambaDM against several baselines in the D4RL benchmark. MambaDM consistently demonstrates superior performance, often securing top-1 and top-2 rankings in various environments. For instance, in the hopper (M) dataset, MambaDM achieves an average return of 85.7, significantly outperforming DT (68.4) and DS4 (54.2). These results underscore MambaDM’s ability to consistently outperform or closely match the top-performing baselines across diverse datasets and tasks, demonstrating its reliability and robustness in continuous RL environments.

### 5.4 Analysis of the Learned Dependencies in MambaDM

It is important to note that in state-space models,  $\bar{\mathbf{A}}$  is defined as a transition matrix parameterized by  $\mathbf{A}$  and  $\Delta$ , with  $\mathbf{A}$  playing a critical role in influencing the stability of the dynamic system [6, 32]. The magnitude of the eigenvalues in  $\mathbf{A}$ ,  $|\lambda_j|$ , is pivotal in determining the range of dependencies captured by the model. If  $|\lambda_j| \geq 1$ , the model can retain historical information across numerous time steps, effectively capturing long-range dependencies. Conversely, when  $|\lambda_j|$  is significantly less than 1, the historical information decays rapidly, leading to a focus on short-term dependencies.

We visualize the key transition matrix  $\mathbf{A}$  in the Mamba block under the Atari domain. For simplified visualization, the eigenvalues of  $\mathbf{A}$  are presented in log-scale. Our analysis reveals two key findings: (1) The distribution of eigenvalues in the Global Mamba varies significantly across different embedding dimensions. As the layers deepen, there is a noticeable trend of increasing eigenvalues, indicating enhanced preservation of long-range information. (2) The eigenvalues in the Local Mamba exhibit a stable distribution across different embedding dimensions and layers, suggesting that the Local Mamba effectively captures both short-range and long-range dependencies. In summary, Figure 3 illustrates how different scale (*i.e.*, global or local) blocks handle varying ranges of dependencies. This highlights the complementary roles of global and local Mamba blocks in processing and preserving multi-scale information within the model.

Method	Embedding Type	Module	Breakout	Qbert	Sequest	Pong
CMC	Cascaded	Mamba & Conv	330.3 $\pm$ 78.8	21.5 $\pm$ 5.5	63.4 $\pm$ 13.7	1.4 $\pm$ 0.1
PMC	Parallel	Mamba & Conv	298.6 $\pm$ 81.7	21.6 $\pm$ 7.6	13.0 $\pm$ 3.8	2.7 $\pm$ 0.1
<b>GLoMa (ours)</b>	Parallel	Mamba only	<b>365.4 <math>\pm</math> 20.0</b>	<b>74.4 <math>\pm</math> 8.4</b>	<b>110.8 <math>\pm</math> 2.3</b>	<b>2.9 <math>\pm</math> 0.1</b>

Table 4: Ablation results of Mamba module combinations. We set up three kinds of mamba methods including Cascaded Mamba-Conv (CMC), Parallel Mamba-Conv (PMC), and our proposed GLoMa.

$A_n$ Initialization	Breakout	Sequest
$A_n = -1/2$	329.8	<b>3.1</b>
$A_n = -(n+1)$	<b>365.4</b>	2.9

Table 5: Ablation results of different initialization of Mamba matrix  $A_n$ .

Context length	10	30	40	60	Mean
DMamba	231.6	239.2	295.9	271.1	259.5
<b>MambaDM</b>	334.4	365.4	325.7	313.2	<b>334.7 (+75.2)</b>

Table 6: Ablation results of different context length  $K$  in Atari Breakout.

Atari	Init RTG	Breakout				Qbert				Pong			
		45	90	900	1800	1000	2500	10000	14000	10	20	100	1000
	Score	194.5	300.3	<b>365.3</b>	337.0	24.4	25.4	<b>45.4</b>	38.6	87.2	106.2	<b>110.8</b>	107.6
OpenAI Gym	Halfcheetah-M					Hopper-M				Walker2d-M			
	Init RTG	2500	5000	10000	50000	1800	3600	7200	36000	6000	12000	24000	240000
	Score	75.3	77.3	<b>78.2</b>	76.9	58.0	81.2	84.9	<b>85.7</b>	42.6	<b>42.8</b>	42.7	<b>42.8</b>

Table 7: Ablation results of MambaDM with different initialized RTG.

## 5.5 Ablation Studies

**Exploration on Mamba Module Combinations.** To design a robust and effective module, we implemented two methods with different embedding configurations (cascaded/parallel) and sub-module choices (mamba/convolution). The results in Table 4 demonstrate that GLoMa significantly outperforms both CMC and PMC on the Atari datasets, confirming the robustness of our MNM design. A detailed analysis of module design is discussed in Appendix A.1.

**Ablations on Mamba initialization.** As demonstrated by Gu et al. [32, 6], the initialization of the state matrix  $A_n$  significantly influences the stability of overall performance, as the eigenvalues of  $A_n$  are closely related to the information transformation process. Consequently, we conduct experiments by varying the initial values of  $A_n$ . The results presented in Table 5 indicate that our MambaDM exhibits stable performance across different initializations.

**Evaluating with different context length.** Mamba has demonstrated strong stability in handling long sequences within NLP tasks [7]. To verify the stability of our proposed method, we evaluate the effect of context length  $K$  compared to DMamba. The results in Table 6 reveal that MambaDM not only maintains stable performance across various context lengths  $K$ , but also achieves significantly improved results, with an average increase of 75.2 points compared to DMamba.

**Ablations on different initialized RTG.** Table 7 explores the impact of different initial return-to-go (RTG) settings on the final performance across various datasets. The results indicate that, generally, as the initial RTG increases, the overall performance of the model improves. However, in specific datasets, such as Breakout, an excessively high initial RTG can negatively affect performance. Overall, the performance of the model is highly correlated with the initial RTG, showing a positive relationship within a certain range. This suggests that while increasing RTG can enhance performance, there is a threshold beyond which the benefits diminish or even reverse. Efficiently determining the optimal RTG setting to avoid extensive experimentation and to enable the model to achieve the best performance is a pertinent area for future research.

## 6 Limitations

First, despite MambaDM achieving SOTA performance, it remains confined to the paradigm of reward-conditional-based supervised learning, ignoring the trajectory stitching capability that affects the sequence model learning from sub-optimal data. We will explore how to select the relative optimal paths and focus on finding the maximum reward path in future work. Second, we observe that the varied target RTG setting results in performance fluctuations. How to determine the optimal RTG is crucial for future work.



## 7 Conclusion

In this study, we proposed the Mamba Decision Maker (MambaDM), a novel action predictor designed to capture multi-scale features and better understand the correlations within RL trajectories. MambaDM leverages a unique global-local fusion mamba (GLoMa) mixer module that adeptly integrates global and local features of input sequences. Extensive experiments have demonstrated that MambaDM achieves state-of-the-art performance on Atari and OpenAI Gym benchmarks. Moreover, our investigation into the scaling laws of MambaDM reveals that increasing the dataset size results in significant performance improvements, underscoring the importance of dataset size over model size in enhancing performance under Atari and OpenAI Gym. In summary, MambaDM presents a promising alternative for sequence modeling in RL, offering efficient multi-scale dependency modeling and paving the way for future advancements in the field.

## References

- [1] L. Chen, K. Lu, A. Rajeswaran, K. Lee, A. Grover, M. Laskin, P. Abbeel, A. Srinivas, and I. Mordatch. Decision transformer: Reinforcement learning via sequence modeling. *NeurIPS*, 34:15084–15097, 2021.
- [2] P.-L. Guhur, S. Chen, R. G. Pinel, M. Tapaswi, I. Laptev, and C. Schmid. Instruction-driven history-aware policies for robotic manipulations. In *CoRL*, pages 175–187. PMLR, 2023.
- [3] M. Shridhar, L. Manuelli, and D. Fox. Perceiver-actor: A multi-task transformer for robotic manipulation. In *CoRL*, pages 785–799. PMLR, 2023.
- [4] D. Shah, A. Bhorkar, H. Leen, I. Kostrikov, N. Rhinehart, and S. Levine. Offline reinforcement learning for customizable visual navigation. In *NeurIPS Workshops*, 2022.
- [5] S. Lifshitz, K. Paster, H. Chan, J. Ba, and S. McIlraith. Steve-1: A generative model for text-to-behavior in minecraft. *NeurIPS*, 36, 2024.
- [6] A. Gu, K. Goel, and C. Re. Efficiently modeling long sequences with structured state spaces. In *ICLR*, 2021.
- [7] A. Gu and T. Dao. Mamba: Linear-time sequence modeling with selective state spaces. *arXiv preprint arXiv:2312.00752*, 2023.
- [8] T. Ota. Decision mamba: Reinforcement learning via sequence modeling with selective state spaces. *arXiv preprint arXiv:2403.19925*, 2024.
- [9] R. S. Sutton and A. G. Barto. Reinforcement learning: An introduction. *Robotica*, 17(2): 229–235, 1999.
- [10] R. S. Sutton and A. G. Barto. The reinforcement learning problem. *Reinforcement learning: An introduction*, pages 51–85, 1998.
- [11] S. Levine, A. Kumar, G. Tucker, and J. Fu. Offline reinforcement learning: Tutorial, review, and Perspectives on Open Problems, 5, 2020.
- [12] S. Fujimoto, D. Meger, and D. Precup. Off-policy deep reinforcement learning without exploration. In *ICML*, pages 2052–2062. PMLR, 2019.
- [13] A. Kumar, A. Zhou, G. Tucker, and S. Levine. Conservative q-learning for offline reinforcement learning. *NeurIPS*, 33:1179–1191, 2020.
- [14] R. Agarwal, D. Schuurmans, and M. Norouzi. An optimistic perspective on offline reinforcement learning. In *ICML*, pages 104–114. PMLR, 2020.

- [15] Y. Wu, S. Zhai, N. Srivastava, J. Susskind, J. Zhang, R. Salakhutdinov, and H. Goh. Uncertainty weighted actor-critic for offline reinforcement learning. *arXiv preprint arXiv:2105.08140*, 2021.
- [16] T. Yu, G. Thomas, L. Yu, S. Ermon, J. Y. Zou, S. Levine, C. Finn, and T. Ma. Mopo: Model-based offline policy optimization. *NeurIPS*, 33:14129–14142, 2020.
- [17] R. Kidambi, A. Rajeswaran, P. Netrapalli, and T. Joachims. Morel: Model-based offline reinforcement learning. *NeurIPS*, 33:21810–21823, 2020.
- [18] A. Argenson and G. Dulac-Arnold. Model-based offline planning. *arXiv preprint arXiv:2008.05556*, 2020.
- [19] S. Depeweg, J. M. Hernández-Lobato, F. Doshi-Velez, and S. Udluft. Learning and policy search in stochastic dynamical systems with bayesian neural networks. *arXiv preprint arXiv:1605.07127*, 2016.
- [20] P. Swazinna, S. Udluft, and T. Runkler. Overcoming model bias for robust offline deep reinforcement learning. *Engineering Applications of Artificial Intelligence*, 104:104366, 2021.
- [21] Y. Ding, C. Florensa, P. Abbeel, and M. Phielipp. Goal-conditioned imitation learning. *NeurIPS*, 32, 2019.
- [22] D. Ghosh, A. Gupta, A. Reddy, J. Fu, C. Devin, B. Eysenbach, and S. Levine. Learning to reach goals via iterated supervised learning. *arXiv preprint arXiv:1912.06088*, 2019.
- [23] C. Lynch, M. Khansari, T. Xiao, V. Kumar, J. Tompson, S. Levine, and P. Sermanet. Learning latent plans from play. In *CoRL*, pages 1113–1132. PMLR, 2020.
- [24] A. Kumar, X. B. Peng, and S. Levine. Reward-conditioned policies. *arXiv preprint arXiv:1912.13465*, 2019.
- [25] J. Schmidhuber. Reinforcement learning upside down: Don’t predict rewards—just map them to actions. *arXiv preprint arXiv:1912.02875*, 2019.
- [26] R. K. Srivastava, P. Shyam, F. Mutz, W. Jaśkowski, and J. Schmidhuber. Training agents using upside-down reinforcement learning. *arXiv preprint arXiv:1912.02877*, 2019.
- [27] S. Emmons, B. Eysenbach, I. Kostrikov, and S. Levine. Rvs: What is essential for offline rl via supervised learning? *ICLR*, 2021.
- [28] M. Siebenborn, B. Belousov, J. Huang, and J. Peters. How crucial is transformer in decision transformer? *arXiv preprint arXiv:2211.14655*, 2022.
- [29] J. Kim, S. Lee, W. Kim, and Y. Sung. Decision convformer: Local filtering in metaformer is sufficient for decision making. In *ICLR*, 2023.
- [30] W. Yu, M. Luo, P. Zhou, C. Si, Y. Zhou, X. Wang, J. Feng, and S. Yan. Metaformer is actually what you need for vision. In *CVPR*, pages 10819–10829, 2022.
- [31] S. B. David, I. Zimmerman, E. Nachmani, and L. Wolf. Decision s4: Efficient sequence-based rl via state spaces layers. In *ICLR*, 2022.
- [32] A. Gu, T. Dao, S. Ermon, A. Rudra, and C. Ré. Hippo: Recurrent memory with optimal polynomial projections. *NeurIPS*, 33:1474–1487, 2020.
- [33] A. Vaswani, N. Shazeer, N. Parmar, J. Uszkoreit, L. Jones, A. N. Gomez, Ł. Kaiser, and I. Polosukhin. Attention is all you need. *NeurIPS*, 30, 2017.

- [34] B. Peng, E. Alcaide, Q. Anthony, A. Albalak, S. Arcadinho, S. Biderman, H. Cao, X. Cheng, M. Chung, L. Derczynski, et al. Rvk: Reinventing rnns for the transformer era. In *EMNLP Findings*, pages 14048–14077, 2023.
- [35] D. Y. Fu, T. Dao, K. K. Saab, A. W. Thomas, A. Rudra, and C. Re. Hungry hungry hippos: Towards language modeling with state space models. In *ICLR*, 2022.
- [36] H. Touvron, T. Lavril, G. Izacard, X. Martinet, M.-A. Lachaux, T. Lacroix, B. Rozière, N. Goyal, E. Hambro, F. Azhar, et al. Llama: Open and efficient foundation language models. *arXiv preprint arXiv:2302.13971*, 2023.
- [37] A. Chowdhery, S. Narang, J. Devlin, M. Bosma, G. Mishra, A. Roberts, P. Barham, H. W. Chung, C. Sutton, S. Gehrmann, et al. Palm: Scaling language modeling with pathways. *JMLR*, 24(240):1–113, 2023.
- [38] L. Zhu, B. Liao, Q. Zhang, X. Wang, W. Liu, and X. Wang. Vision mamba: Efficient visual representation learning with bidirectional state space model. *arXiv preprint arXiv:2401.09417*, 2024.
- [39] Y. Liu, Y. Tian, Y. Zhao, H. Yu, L. Xie, Y. Wang, Q. Ye, and Y. Liu. Vmamba: Visual state space model. *arXiv preprint arXiv:2401.10166*, 2024.
- [40] Y. Teng, Y. Wu, H. Shi, X. Ning, G. Dai, Y. Wang, Z. Li, and X. Liu. Dim: Diffusion mamba for efficient high-resolution image synthesis. *arXiv preprint arXiv:2405.14224*, 2024.
- [41] M. Pióro, K. Ciebia, K. Król, J. Ludziejewski, and S. Jaszczur. Moe-mamba: Efficient selective state space models with mixture of experts. *ICLR Workshops*, 2024.
- [42] Q. Anthony, Y. Tokpanov, P. Glorioso, and B. Millidge. Blackmamba: Mixture of experts for state-space models. *arXiv preprint arXiv:2402.01771*, 2024.
- [43] J. Liu, H. Yang, H.-Y. Zhou, Y. Xi, L. Yu, Y. Yu, Y. Liang, G. Shi, S. Zhang, H. Zheng, et al. Swin-umamba: Mamba-based unet with imagenet-based pretraining. *arXiv preprint arXiv:2402.03302*, 2024.
- [44] Z. Xing, T. Ye, Y. Yang, G. Liu, and L. Zhu. Segmamba: Long-range sequential modeling mamba for 3d medical image segmentation. *arXiv preprint arXiv:2401.13560*, 2024.
- [45] K. Han, A. Xiao, E. Wu, J. Guo, C. Xu, and Y. Wang. Transformer in transformer. *NeurIPS*, 34:15908–15919, 2021.
- [46] N. Srivastava, G. Hinton, A. Krizhevsky, I. Sutskever, and R. Salakhutdinov. Dropout: a simple way to prevent neural networks from overfitting. *JMLR*, 15(1):1929–1958, 2014.
- [47] V. Mnih, K. Kavukcuoglu, D. Silver, A. Graves, I. Antonoglou, D. Wierstra, and M. Riedmiller. Playing atari with deep reinforcement learning. *arXiv preprint arXiv:1312.5602*, 2013.
- [48] J. Fu, A. Kumar, O. Nachum, G. Tucker, and S. Levine. D4rl: Datasets for deep data-driven reinforcement learning. *arXiv preprint arXiv:2004.07219*, 2020.
- [49] J. Kaplan, S. McCandlish, T. Henighan, T. B. Brown, B. Chess, R. Child, S. Gray, A. Radford, J. Wu, and D. Amodei. Scaling laws for neural language models. *arXiv preprint arXiv:2001.08361*, 2020.
- [50] W. Ye, S. Liu, T. Kurutach, P. Abbeel, and Y. Gao. Mastering atari games with limited data. *NeurIPS*, 34:25476–25488, 2021.
- [51] M. Bain and C. Sammut. A framework for behavioural cloning. In *Machine Intelligence*, pages 103–129, 1995.

- [52] S. Fujimoto and S. S. Gu. A minimalist approach to offline reinforcement learning. *NeurIPS*, 34:20132–20145, 2021.
- [53] I. Kostrikov, A. Nair, and S. Levine. Offline reinforcement learning with implicit q-learning. In *ICLR*, 2021.
- [54] L. Gao, J. Schulman, and J. Hilton. Scaling laws for reward model overoptimization. In *International Conference on Machine Learning*, pages 10835–10866. PMLR, 2023.
- [55] P. Bhargava, R. Chitnis, A. Geramifard, S. Sodhani, and A. Zhang. When should we prefer decision transformers for offline reinforcement learning? In *ICLR*, 2024. URL <https://openreview.net/forum?id=vpV7f0FQy4>.
- [56] M. G. Bellemare, Y. Naddaf, J. Veness, and M. Bowling. The arcade learning environment: An evaluation platform for general agents. *JAIR*, 47:253–279, 2013.
- [57] V. Mnih, K. Kavukcuoglu, D. Silver, A. A. Rusu, J. Veness, M. G. Bellemare, A. Graves, M. Riedmiller, A. K. Fidjeland, G. Ostrovski, et al. Human-level control through deep reinforcement learning. *Nature*, 518(7540):529–533, 2015.
- [58] G. Brockman, V. Cheung, L. Pettersson, J. Schneider, J. Schulman, J. Tang, and W. Zaremba. Openai gym. *arXiv preprint arXiv:1606.01540*, 2016.

# Appendix

## A Discussion

### A.1 Global-local Module Design

Our model is designed with a parallel architecture that includes a global branch and a local branch. The global branch extracts global information within the RL trajectory, while the local branch focuses on local information based on the Markov Decision Process (MDP). To better validate the effectiveness of our design, we tried some other reasonable modules as illustrated in Figure 4. As claimed in the Decision ConvFormer [29], due to the MDP, the current and previous features are critical, and convolutional operations can effectively extract such local information. Therefore, we replaced our local branch with the convolutional module from DC to create the Parallel Mamba-Conv (PMC). However, as shown in Table 4, PMC did not yield satisfactory results, demonstrating that the convolutional operation is not suited to extract local features when cooperating with Mamba. Additionally, considering that the processing order may affect performance, we designed a coarse-to-fine cascaded Mamba-Conv (CMC) structure. This approach aimed to first extract global features and then refine local features, but the results for CMC were also suboptimal, as shown in Table 4.

Furthermore, we compared the Decision Transformer [1] with its variants, Decision ConvFormer [29] and Decision Mamba [8], as illustrated in Figure 4d-f. From our perspective, these models focus on explicitly capturing one kind of feature (global/local) in sequence. Although these models have shown commendable performance, our proposed GLoMa module is specifically tailored for capturing the global and local correlations to better understand the inner relationships in RL trajectories. Therefore, our module design is well-justified, and the results in the main text indicate that our model achieved the best performance, thereby demonstrating its effectiveness.

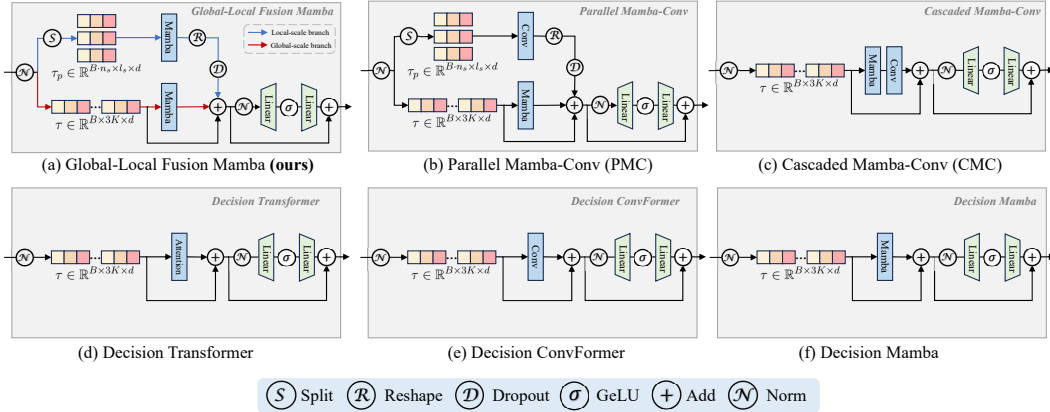


Figure 4: Visualization of different module designs. We designed the (a) **GLoMa** tailored for capturing global and local information in RL sequences. (b) Parallel Mamba-Conv is designed to demonstrate that the convolutional operation is not suited for extracting local features when used in conjunction with Mamba. (c) Cascaded Mamba-Conv aims to test which feature capture order (cascade/parallel) is more effective. We also provide illustrations of the baselines: (d) Decision Transformer, (e) Decision ConvFormer, and (f) Decision Mamba.

### A.2 Exploration on RL scaling laws

In this paper, we conduct extensive experiments to explore the scaling laws in certain RL environments: Atari and OpenAI Gym. Our results indicate that: increasing the model size does not lead to performance improvements and may even have negative effects. However, increasing the dataset size can significantly enhance model performance. Based on these findings, we discuss the following points:

- **Model Size Scaling:** Our experimental results diverge from the scaling laws observed in natural language processing (NLP), as enlarging the model size did not yield performance gains. This discrepancy may be attributed to several factors: (1) The model size is strongly correlated with its capability, but the optimal model size varies across different RL tasks. Our experiments are limited to two standard RL datasets, which may not provide a com-

prehensive understanding of scaling behavior across diverse RL tasks. (2) RL trajectories possess different attributes compared to text data, despite Mamba showing scaling law behaviors in NLP tasks [7].

- **Dataset Size Scaling:** Increasing the dataset size enhances model performance. This empirical conclusion aligns with findings from existing studies [54, 55]. These studies suggest that larger datasets provide richer experiences for the model to learn from, improving generalization and robustness.

In summary, we recommend that: For Atari and OpenAI Gym tasks, increasing the model size is not necessarily beneficial. Instead, expanding the dataset size is potentially advantageous, as it helps avoid over-optimization [54] and improves overall model performance. Future work aims to expand our analysis across more varied RL datasets and explore additional factors that may influence the scaling properties of MambaDM.

## B Experiment Details

### B.1 Atari

**Dataset Introduction.** The Atari domain is built upon a collection of classic video games [47] and is an essential testbed for evaluating reinforcement learning algorithms due to the challenge of delayed rewards, which obscure the direct correlation between specific actions and their outcomes. This characteristic makes it ideal for assessing an agent’s skill in long-term credit assignments. In particular, the DQN Replay Dataset includes replay data from the training of a DQN agent across 60 Atari 2600 games [56], capturing approximately 50 million experience tuples of observations, actions, rewards, and next observations, thus supporting extensive offline reinforcement learning research. In our experiments, we utilized Atari datasets provided by Agarwal et al. [14], constituting 1% of all samples (*i.e.*, 500K) in the replay data generated during the training of a DQN agent [57]. We conducted experiments in eight games: Breakout, Qbert, Pong, Seaquest, Asterix, Frostbite, Assault, and Gopher, using these datasets to benchmark the performance of our method.

**Hyperparameter Settings.** We adopt the same basic experimental settings as used in Decision Transformer [1], with detailed hyperparameter configurations summarized in Table 8. We set the random seeds as {123, 231, 312}. Similar to Agarwal et al. [14], the main results of our model are trained on 1% samples in the DQN-replay datasets, which equates to 500K transitions [57]. Following Kim et al. [29], we also utilize the context length settings detailed in Table 9. As highlighted in our main experiment, the initial return-to-go (RTG) significantly impacts final performance. Therefore, we examine four target RTG values (listed in Table 9), each being a multiple of the default target RTG, and report the highest score in the main results table.

**Atari Task Scores.** In the main text, we report the normalized scores (*i.e.*,  $100 \times (\text{score}_{\text{raw}} - \text{score}_{\text{random}}) / (\text{score}_{\text{expert}} - \text{score}_{\text{random}})$ ) for each domain, calculated using baseline random and expert scores, as shown in Table 10. This methodology follows the approach in [50, 57].

### B.2 OpenAI Gym

**Dataset Introduction.** In this paper, we focus on the locomotion tasks from the D4RL benchmark [48] as implemented in OpenAI Gym [58]. These tasks are critical for developing and evaluating reinforcement learning algorithms in continuous control settings. We utilize several specific environments within the locomotion category, including `halfCheetah`, `hopper`, and `walker2D`, each designed to test different aspects of control and coordination.

- `HalfCheetah`: A two-dimensional bipedal robot designed to run as fast as possible.
- `Hopper`: A single-legged robot that aims to hop forward without falling.
- `Walker2D`: A two-dimensional bipedal robot aiming to walk as far as possible without falling.

Each of these environments has three distinct dataset settings designed to test different aspects of algorithm performance:

- **Medium:** 1 million timesteps generated by a policy that achieves approximately one-third the score of an expert policy.



Hyperparameter	Value
Number of layers	6
Embedding dimension	128
Mamba expand size	1
Batch size	256
Return-to-go conditioning	90 Breakout ( $\approx 1 \times$ max in dataset) 2500 Qbert ( $\approx 5 \times$ max in dataset) 20 Pong ( $\approx 1 \times$ max in dataset) 1450 Seaquest ( $\approx 5 \times$ max in dataset) 520 Asterix ( $\approx 5 \times$ max in dataset) 950 Frostbite ( $\approx 5 \times$ max in dataset) 780 Assault ( $\approx 5 \times$ max in dataset) 2750 Gopher ( $\approx 5 \times$ max in dataset)
Nonlinearity	ReLU, encoder GELU, otherwise
Encoder channels	32, 64, 64
Encoder filter sizes	$8 \times 8, 4 \times 4, 3 \times 3$
Encoder strides	4, 2, 1
Max epochs	10
Dropout	0.1
Learning rate	$6 \times 10^{-4}$
Adam betas	(0.9, 0.95)
Grad norm clip	1.0
Weight decay	0.1
Learning rate decay	Linear warmup and cosine decay
Warmup tokens	512 * 20
Final tokens	2 * 500000 * $K$

Table 8: Hyperparameters of MambaDM on the Atari domain.

Game	Context length $K$	Target RTG
Breakout	30	{45, 90, 900, 1800}
Qbert	30	{1000, 2500, 10000, 14000}
Pong	50	{10, 20, 100, 1000}
Seaquest	30	{500, 1150, 1450, 6000}
Asterix	30	{200, 520, 1000, 2500}
Frostbite	30	{475, 950, 2000, 5000}
Assault	30	{390, 780, 1600, 3200}
Gopher	30	{1375, 2750, 5000, 10000}

Table 9: The context length  $K$  and target RTG when training MambaDM on the Atari domain.

- **Medium-Expert:** 1 million timesteps generated by the medium policy concatenated with 1 million timesteps generated by an expert policy.
- **Medium-Replay:** The replay buffer of an agent trained to the performance of a medium policy, covering approximately 25k-400k timesteps.

**Hyperparameter Settings.** Similarly, we adopt the same basic experimental settings as used in Decision Transformer [1], with detailed hyperparameter configurations summarized in Table 11. We set the random seeds as {123, 231, 312}. The length settings and the target RTG settings are detailed in Table 12.

Game	Random	Expert
Breakout	1.7	30.5
Qbert	163.9	13455.0
Pong	-20.7	14.6
Seaquest	68.4	42054.7
Asterix	210.0	8503.3
Frostbite	65.2	4334.7
Assault	222.4	742.0
Gopher	257.6	2412.5

Table 10: The mean and variance of raw scores for the 1% DQN-replay Atari datasets across three seeds. “Random” and “Expert” indicate the Atari baseline scores used for normalization.

Hyperparameter	Value
Number of layers	3
Batch size	64
Embedding dimension	128
Mamba expand size	1
Context length $K$	20
Return-to-go conditioning	6000 HalfCheetah 3600 Hopper 5000 Walker2D
Dropout	0.1
Nonlinearity function	GeLU
Grad norm clip	0.25
Weight decay	$10^{-4}$
Learning rate decay	Linear warmup
Warmup step	10000
Learning rate	$10^{-4}$
Total number of updates	$10^5$

Table 11: Hyperparameters of MambaDM on the OpenAI Gym.

Game	Context length $K$	Target RTG
halfcheetah	20	{1800, 3600, 7200, 36000, 72000}
hopper	20	{6000, 12000, 24000, 120000, 240000}
walker2D	20	{2500, 5000, 10000, 50000, 100000}

Table 12: The context length  $K$  and target RTG when training MambaDM on the OpenAI Gym.